

Automated Machine Learning can Classify Bound Entangled States with Tomograms

Caio B. D. Goes,¹ Askery Canabarro,^{2,3} Eduardo I. Duzzioni,¹ and Thiago O. Maciel¹

¹*Departamento de Física, Universidade Federal de Santa Catarina, 88040-900, Florianópolis, SC, Brazil*

²*International Institute of Physics, Federal University of Rio Grande do Norte, 59078-970, Natal, RN, Brazil*

³*Grupo de Física da Matéria Condensada, Núcleo de Ciências Exatas - NCEX,*

Campus Arapiraca, Universidade Federal de Alagoas, 57309-005, Arapiraca, AL, Brazil

(Dated: July 6, 2022)

For quantum systems with total dimension greater than six, the positive partial transposition (PPT) criterion is necessary but not sufficient to decide the non-separability of quantum states. Here, we present an Automated Machine Learning approach to classify random states of two qutrits as separable or entangled even when the PPT criterion fails. We successfully applied our framework using enough data to perform a quantum state tomography and without any direct measurement of its entanglement. In addition, we could also estimate the Generalized Robustness of Entanglement with regression techniques and use it to validate our classifiers.

I. INTRODUCTION

Entanglement is critical for real-world Quantum Information protocols like Quantum Computation [1, 2] and Unconditionally Secure Quantum Cryptography [3–5]. In this context, non-separable systems with local dimensions with more than two degrees of freedom are especially important due to its tolerance to noise [5].

For quantum systems with total dimension up to six (*e.g.*, two qubits or one qubit and one qutrit), the so-called Peres-Horodecki's *Positive Partial Transposition* (PPT) criterion [6, 7] is necessary and sufficient. For larger systems, the criterion is sufficient but not necessary and we have entangled states with positive partial transposition [8]. We can find several examples of PPT entangled states (PPTES), also known as bound entangled states, in the literature [8–13].

Although we can decide whether a quantum state has *Negative Partial Transposition* (NPT) or PPT within a polynomial number of operations, there is no operational necessary and sufficient criterion for the separability problem in general, moreover, Gurvits proved this decision problem to be NP-HARD [14, 15].

In case we are willing to pay the computational effort, we can choose an *Entanglement Witness* (EW) [7] for entanglement detection. In terms of experimental setups, we can implement EWs when we have partial information about the state (*cf.* the references in [16]), but they are not attractive, since each state has its own optimal witness.

It is not difficult to imagine real-world scenarios in which we will need to decide whether our quantum states are entangled or not in a very short time window. In spite of having numerous schemes to infer entanglement with partial information [17–20], they usually rely on EWs, especially when we have PPTES. In such time-sensitive scenarios, spending hours to compute optimal entanglement witnesses (OEW) is a luxury, so here we advocate the use of *Machine Learning* (ML) techniques to characterize entanglement in an efficient post-processing manner, keeping the data gathering as simple as possible.

ML techniques have recently become attractive tools to explore quantum mechanics in different problems [21], for instance, there are successful applications in problems like quantum tomography [22, 23], quantum error correction [24, 25], quantum control [26], assessment of NPT entanglement through Bell inequalities [27–29], and quantum phase transitions [30]. In a nutshell, ML is used to build complex models capable of making predictions about difficult problems [31], such as the separability problem described above.

Differently from [27, 28], here we investigate how ML tools deal with harder instances of the classification of entanglement between two qutrits. More specifically, we do not consider a particular family of states with a small number of coefficients, we have a list of randomly drawn states classified as separable (SEP), entangled with positive partial transposition (PPTES), and entangled with negative partial transposition (NPT).

With this list, we chose a scenario in which we possess enough data to perform a quantum tomography of a state ρ via linear system inversion [32], but no direct measurements of its entanglement. The idea was first assess the possibility of using a fewer number of coefficients, but it was not possible for random states. Using all coefficients, we applied supervised ML techniques to infer a function that best maps the tomograms to our labels (SEP/PPTES/NPT). In spite of including NPT states in the list, we are particularly interested in the hardest instance of the problem: where Peres-Horodecki criterion cannot decide between SEP/PPTES. For this task, we chose *Automated Machine Learning* (autoML) schemes [33–36] and evaluated their performances in this decision problem.

The computational effort to construct this training dataset is herculean, but it pays off when, after the completion of a successfully model, we can decide if a state ρ is SEP/PPTES and SEP/PPTES/NPT with high probability. In addition, we could also estimate the amount of entanglement in the state using autoML for the regression task of an entanglement quantifier, namely, the Generalized Robustness of Entanglement [37, 38].

This paper is organized as follows: in Sec. II, we

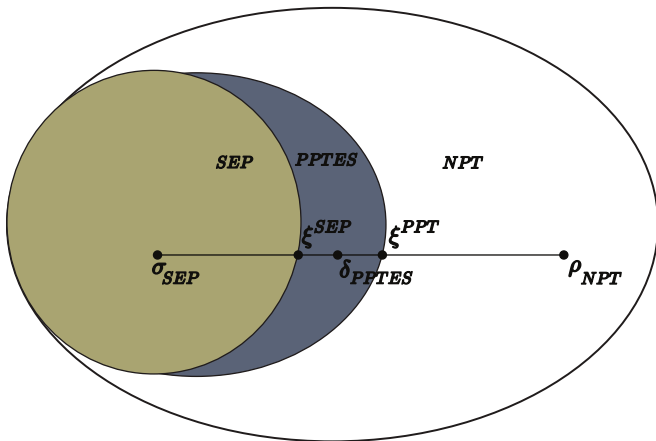


FIG. 1. Schematic representation of state space with separable states (SEP) σ_{SEP} , entangled states with Positive Partial Transposition (PPTES) δ_{PPTES} , and states with Negative Partial Transposition (NPT) ρ_{NPT} . We also have edge states ξ^{SEP} and ξ^{PPT} lying in the frontier between SEP/PPTES and PPTES/NPT, respectively.

thoroughly explain our methodology for constructing our dataset; in Sec. III, we explain the automated machine learning and its advantages; in Sec. IV, we discuss our results and, finally in Sec. V, we conclude and give some future perspectives.

II. DATASET

Choosing the right methodology to construct a training dataset is crucial to the quality of the results [39] in any ML task. Sampling random mixed states of a given dimension can be non-trivial for different reasons: (i) we need to specify a probability measure on the set of all density operators of this dimension [40]; (ii) the volume of separable (SEP), entangled states with positive partial transposition (PPTES) and entangled states with negative partial transposition (NPT) are not the same [41–43]; (iii) there is no operational necessary and sufficient criterion for the separability problem in general.

Our methodological choices for these issues were the following: (i) we chose to sample our mixed states using the Hilbert-Schmidt measure [44, 45]; (ii) since SEP, PPTES and NPT sets have different volumes, we chose to use the same number of examples in each class; (iii) we first split between NPT/PPT using the Peres-Horodecki criterion [46] and, within the PPT, we decided between PPTES/SEP using ϵ -Optimal Entanglement Witnesses (ϵ -OEW) [47, 48] to compute the *Generalized Robustness of Entanglement* (GR) [37, 38].

We opt for (ii) to balance our dataset, otherwise we would have a small number of SEP and PPTES in the sample [41]. Since the probability of randomly draw a PPTES is low, we used two strategies to sample in this set, explained in the next sections.

It is worth to note that this work differs from [27, 28] in several aspects. Beside the choice of using random states, we also used a different choice of non-separability tests when Peres-Horodecki criterion fails. We chose EWs instead of Doherty *et al.* [49] k -separability hierarchy so we could estimate the amount of entanglement in the state ρ for further use in the regression test. We also had numerical evidence that using just the lower level ($k = 2$) of the hierarchy lead to even lower probability of asserting PPTES of randomly drawn states, with no addition to the performance in Section IV.

A. Dataset with random states of two qutrits

Suppose we draw a random state $\rho \in \mathcal{D} \subset \mathcal{L}(\mathbb{C}^3 \otimes \mathbb{C}^3)$, where \mathcal{D} is the state space, and \mathcal{L} is the set of linear operators in the Hilbert space $\mathcal{H} \simeq \mathbb{C}^3 \otimes \mathbb{C}^3$.

We can write ρ as

$$\rho = \sum_{i=1}^{d^2-1} \theta_i E_i, \quad (1)$$

where E_i form a basis in Hilbert-Schmidt space and θ_i is the solution to the following linear system [32]:

$$G^{-1}\vec{c} = \vec{\theta}, \quad G_{ij} = \text{tr}(E_i E_j), \quad c_i = \text{tr}(E_i \rho). \quad (2)$$

We can choose any basis as long as it spans the Hilbert-Schmidt space. Here, we want to avoid measurements on entangled projectors, so we chose the $SU(3) \otimes SU(3)$ generators to simplify the measurement requirements.

The Generalized Robustness (GR) [37, 38] is an entanglement quantifier obtainable via entanglement witnesses [47, 48]. GR is the minimal amount of mixing with any state needed to destroy the entanglement in ρ , *i.e.*,

$$GR(\rho) = \min_{\sigma \in \mathcal{D}} \left(\min_{s \geq 0 \in \mathbb{R}} s : \xi^{SEP} \equiv \frac{\rho + s\sigma}{1+s} \in SEP \right), \quad (3)$$

where ξ^{SEP} belongs to the edge between separable and entangled states (*cf.* Fig 1). Our ϵ -OEW for GR guarantees that ρ is entangled iff $GR(\rho) > \epsilon$, here we chose $\epsilon = 10^{-5}$.

For our learning process, we encoded ρ in the real vector $\vec{c} \in \mathbb{R}^{d^2-1}$ (*cf.* Eq. (2)). For better adherence to real world applications, we chose tomographic measurements, guaranteeing we have all needed information of ρ but not direct measurements of its entanglement.

We can summarize the algorithm to generate our dataset as follows:

1. Draw a random density matrix ρ according to the Hilbert-Schmidt measure;
2. Compute $GR(\rho)$ using an ϵ -OEW and obtain its edge state ξ^{SEP} ;
3. Check whether ρ is a PPT state;

4. If ρ is PPT and $GR(\rho) > \epsilon$, we save ρ in our dataset as PPTES;
5. If ρ is PPT and $GR(\rho) \leq \epsilon$, we save ρ in our dataset as SEP;
6. If ρ is NPT and $GR(\rho) > \epsilon$, we save ρ in our dataset as NPT;
7. Encode ρ in \vec{c} using Eqs. (1) and (2) choosing $SU(3) \otimes SU(3)$ generators.

B. Dataset with artificial PPTES

As we know that the probability of drawing a PPTES is low, another possible strategy is to increase the odds using what we call *artificial PPTES* via edge states [50].

In this methodology, we compute *Optimal Decomposable Witnesses* (d-OEW) [48, 51] for the GR, obtaining the edge state ξ^{PPT} , lying in the frontier between PPT and NPT sets (*cf.* Fig 1). We say this is the minimal amount of mixing with any state required to become a PPT state.

Cases where $\xi^{SEP} \neq \xi^{PPT}$ are particularly useful, since we can obtain a PPTES with any convex combination between them [50] (*cf.* Fig 1). We say they are different in trace-norm given a tolerance of 10^{-3} .

Thus, we can summarize the algorithm to generate our dataset as follows:

1. Draw a random density matrix ρ according to the Hilbert-Schmidt measure;
2. Compute $GR(\rho)$ using an ϵ -OEW and obtain its edge state ξ^{SEP} ;
3. Check whether ρ is a PPT state;
4. If ρ is PPT and $GR(\rho) > \epsilon$, we save ρ in our dataset as PPTES;
5. If ρ is PPT and $GR(\rho) \leq \epsilon$, we save ρ in our dataset as SEP;
6. If ρ is NPT and, consequently, $GR(\rho) > \epsilon$, we save ρ in our dataset as NPT.
7. If ρ is NPT, we also quantify $GR(\rho)$ computing an (d-OEW) and its edge state ξ^{PPT} ;
8. Check whether ξ^{SEP} and ξ^{PPT} are different in trace norm, *e.g.*, $\frac{1}{2}\|\xi^{SEP} - \xi^{PPT}\|_1 > 10^{-3}$;
9. If they are different, we have $\delta = \frac{1}{2}\xi^{PPT} + \frac{1}{2}\xi^{SEP}$ and save it as PPTES.
10. Compute $GR(\delta)$ using an ϵ -OEW;
11. If $GR(\delta) > \epsilon$ we save δ in our dataset as PPTES;

Since we are including artificially created PPTES in addition to randomly drawn ones, we need to assess whether we have a fair sample in this subset. In Tab. I, we have the average fidelities,

$$F(\rho, \sigma) = \left[\text{tr} \left(\sqrt{\sqrt{\rho} \sigma \sqrt{\rho}} \right) \right]^2,$$

over states in our dataset. Note a similar average fidelity of PPTES comparing with separable states and, as expected, NPT states are more distant since they have a larger volume in Hilbert space [41].

Class	$\langle F \rangle$
Sample	0.7879
SEP	0.7955
PPTES	0.7965
NPT	0.7712

TABLE I. Average fidelity $\langle F \rangle$ between states in the sample.

The final dataset consists of 3254 states of each class in the triple (SEP/PPTES/NPT), with half random and half artificial PPTES, totaling 9762 states. Although we could benefit from a larger dataset, it took about a month using a cluster of 18 cores and 90GB of RAM to sample ten thousand random states and calculate their ϵ -OEW within the desired numerical precision.

III. AUTOMATED MACHINE LEARNING

Automated Machine Learning (autoML) stands for the automation of some or even all of the following tasks in the ML workflow: feature engineering; model tuning; ensembling; and model deployment. Open source projects such as TPOT [33], auto-sklearn [34], AutoKeras [35], and Auto-PyTorch [36] are common tools used in this endeavor. It is not an exaggeration saying that autoML is a form of learning about learning [52].

We have a threefold motivation to use autoML: (i) we are dealing with a proved NP-HARD problem without a huge dataset; (ii) autoML can provide useful insights about specific tasks, such as different pre-processing schemes; (iii) autoML has a good cost-benefit in terms of implementation time and performance.

(i) is the crux of the matter, so automatically trying different learning algorithms and architectures is paramount to achieve optimum performance [53]. (ii) although autoML was designed for non-experts, an experienced modeller can extract important insights when analyzing partial results, such as the need for *Principal Component Analysis* (PCA) [54], feature importance, and so on. Finally, (iii) was achieved with good accuracy and precision within a few hours of training and a couple of minutes to implement it.

Here, we used supervised learning methods, in which we know the output for each input in the sample, with

the goal of inferring a function that best maps inputs to outputs. Common supervised learning tasks are: (i) classification, when one needs to map input to discrete output (labels), or (ii) regression, when one seeks to map input to a continuous output set. Typical supervised learning algorithms include: Logistic Regression (LR) [55], Naive Bayes (NB) [56], Support Vector Machines (SVM) [57, 58], K-Nearest Neighbour (KNN) [59], Decision Tree (DT) [60], Extreme Gradient Boosting (XGB) [61], Random Forest (RF) [62], and Artificial Neural Networks (ANN) [63], to cite a few. Our autoML schemes received data points from features \mathbf{X} with corresponding target vector \mathbf{y} , and modeled the conditional probability $p(\mathbf{y}|\mathbf{X})$, resulting in a general rule mapping $\mathbf{X} \rightarrow \mathbf{y}$.

In the next section, we have results for three different tasks: (i) binary classification of PPT states of two qutrits as SEP or entangled with positive PPTES; (ii) multi-classification of SEP vs PPTES vs NPT; and (iii) a regression learning of the Generalized Robustness (GR), an entanglement quantifier defined in Eq. (3). Although (iii) seems a completely different problem, we can see a regression task as a classification using a discretized continuous target [64]. So, we can use this regression to estimate the amount of entanglement in the quantum state and validate our classifiers.

IV. RESULTS AND DISCUSSION

A. Feature Importance

In the previous section, we mentioned the possibility of extracting valuable insights when analyzing partial results using autoML. For example, we can use TPOT [33] for feature importance analysis. TPOT runs a genetic program to explore different pipelines given the raw input and output. It automatically runs standard tests, *e.g.*, analysis of data type, z -score, check the relevance of higher powers of the inputs, dimensionality reduction via PCA, hyper-parameters optimization, and so on. It is a good entry point for any autoML project, since we can investigate if one feature is more relevant than the others, which is crucial to diminish the number of used features in a learning process, reducing the computational effort and increasing the robustness against over-fitting [53].

We tested the feature importance of our dataset using TPOT with 10 generations and a population size of 30. The optimization took about 6 hours to conclude using a standard PC and we confirmed that all 80 features contribute equally to solve the problem. Therefore, we cannot reduce the dimensionality of the data without losing considerable information. Since our features c_i (from Eq. (2) represents the inner product of ρ against linearly independent observables ($SU(3) \otimes SU(3)$ generators), this result is expected.

This stress the difference when using random states to train machines capable of discerning between unknown coefficients. In case we want to analyze a family of states

ML technique	Test (%)	PPTES (%)	SEP (%)
TPOT	75.3	76.6	74.1
auto-sklearn	73.4	71.9	75.0
AutoKeras	41.6	40.0	36.0
Auto-PyTorch	62.2	63.7	60.8
AdaBoost	66.9	65.7	68.1
ANN	58.4	57.0	59.9
SVM	70.5	67.1	73.7
KNN	48.4	0.2	99.8
DT	53.0	49.6	56.5
RF	70.3	73.2	67.4

TABLE II. Testing performance for different ML techniques using the same dataset for the binary classification SEP *vs.* PPTES. We show the best performing one in boldface. The autoML techniques are TPOT, auto-sklearn, AutoKeras and Auto-PyTorch. The conventional methods are ensemble method AdaBoost, artificial neural network (ANN), support vector machine (SVM), K-nearest neighbors (KNN), decision tree (DT), and random forest (RF).

composed of fewer parameters, the problem simplifies enormously and it is possible to achieve excellent results [27, 28].

For the classification tests, in addition to the features of the vector $\vec{c} \in \mathbb{R}^{80}$, we also included its exponentials, $\exp(c_i) \forall i = 1, \dots, 80$ and the second-order terms, $c_i \cdot c_j \forall i = 1, \dots, 80$ and $j = i, \dots, 80$, totalling 3400 features. All features were standardized to z -scores, *i.e.*, centered to have zero mean and scaled to have standard deviation of one.

B. Binary Classification (SEP *vs.* PPTES)

After deciding the features, the first task is training binary classifiers to discern between separable and entangled states with positive partial transposition. This is especially important when the Peres-Horodecki criterion fails and we need to decide whether ρ is entangled.

To assess the overall performance of each classifier, we split the dataset in two parts: $\sim 80\%$ for training and $\sim 20\%$ for testing. The idea is to test a trained model with “new information”, so we can ensure the model’s robustness against over-fitting. Thus, we say we have a good model when it achieves a high performance in the testing phase.

We trained different models using different ML techniques within a time window of 6 hours in a standard PC. Their testing performances are in Tab. II, with the best model in boldface. Notice that all autoML strategies (TPOT, auto-sklearn, AutoKeras, Auto-PyTorch, and AdaBoost) outperformed standard algorithms (ANN, SVM, KNN, DT, and RF). In the testing step, TPOT classified SEP with 74.1% accuracy and PPTES with 76.6%, with a overall performance of 75.3%. The *Confusion Matrix* (CM) [31] for this test is in Fig. 2.

Output Class	PPTES	469 36.0%	179 13.7%	72.4% 27.6%
	SEP	143 11.0%	511 39.2%	78.1% 21.9%
		76.6% 23.4%	74.1% 25.9%	75.3% 24.7%
		PPTES	SEP	
		Target Class		

FIG. 2. The testing Confusion Matrix of TPOT classifier. The rows correspond to the output classes (SEP/PPTES) and the columns to the true classes (also SEP/PPTES), having the correctly classified inputs in the diagonal entries and the incorrectly classified in the off-diagonal, with both number of states and percentage of the total number of observations. The last row and column show the percentages of all states predicted to belong to each class that are (in)correctly classified. TPOT achieved an overall performance of 75.3%.

We faced over-fitting in all models due to the curse of dimensionality and the limited amount of data [53]. In some cases, we could get close to 100% accuracy in the training step, but with terrible performance in the testing phase. Nonetheless, the accuracy of about 75.3% for out-of-sample data using TPOT indicates that ML can be a potential new tool to investigate bound entanglement in high-dimensional systems.

C. Multi-classification (SEP vs. PPTES vs. NPT)

Although we can check whether a quantum state is PPT/NPT efficiently, after the successful classification in the previous section, we want to investigate one more class in our autoML framework for a complete entanglement description of two qutrits. The task at hand is a trinary classification of separable, entangled states with positive partial transposition and entangled states with negative partial transposition.

For this task, we split the dataset in $\sim 80\%$ for training and $\sim 20\%$ for testing, and run the same algorithms from the previous section within a time window of 6 hours in a standard PC. We present the results in Tab. III with the best model in boldface. Notice that TPOT still

outperforms other strategies, accurately classifying SEP with 71.4%, PPTES 62.4%, and NPT with 88.6%, with an overall performance of 73.8%. Its confusion matrix for the testing phase is in Fig. 3.

Output Class	NPT	552 28.3%	90 4.6%	3 0.2%	85.6% 14.4%
	PPTES	62 3.2%	418 21.4%	186 9.5%	62.8% 37.2%
	SEP	9 0.5%	162 8.3%	471 24.1%	73.4% 26.6%
		88.6% 11.4%	62.4% 37.6%	71.4% 28.6%	73.8% 26.2%
		NPT	PPTES	SEP	
		Target Class			

FIG. 3. The testing Confusion Matrix of TPOT classifier. The rows correspond to the output classes (SEP/PPTES/NPT) and the columns to the true classes (also SEP/PPTES/NPT), having the correctly classified inputs in the diagonal entries and the incorrectly classified in the off-diagonal, with both number of states and percentage of the total number of observations. The last row and column show the percentages of all states predicted to belong to each class that are (in)correctly classified. TPOT achieved an overall performance of 73.8%.

It is impressive how TPOT and auto-sklearn could deal with the curse of dimensionality, achieving an outstanding accuracy for this challenging scenario. The classification set has now several boundaries (*cf.* Fig. 1): between SEP and PPTES; PPTES and NPT; and between SEP and NPT¹. A reduction of the overall performance was expected, especially with a high-dimensional dataset, possessing 3400 features, and 9762 samples. We noticed a poor performance only in the deep learning (DL) autoML methods, known to need a large amount of instances to achieve a convergence [31]. Notwithstanding, with overall accuracy of 73.8% for out-of-sample data using TPOT indicates that ML can be a potential new tool to investigate bound entanglement in high-dimensional systems.

¹ Werner states [65] is a one-parameter family from SEP to NPT without passing through PPTES.

ML technique	Test (%)	NPT (%)	PPTES (%)	SEP (%)
TPOT	73.8	88.6	62.4	71.4
auto-sklearn	71.9	86.1	53.2	77.2
AutoKeras	52.5	53.0	44.5	54.9
Auto-PyTorch	42.7	68.7	14.0	45.1
AdaBoost	64.2	95.6	48.1	73.5
ANN	56.0	70.3	42.4	55.6
SVM	72.9	86.5	53.7	69.6
KNN	34.1	0.4	0.6	99.6
DT	43.1	48.0	35.1	45.9
RF	69.2	85.0	45.6	76.4

TABLE III. Different machine learning techniques applied to the dataset and the corresponding accuracy for the multi-classification. We show the best performing one in boldface. The autoML techniques are TPOT, auto-sklearn, AutoKeras, and Auto-PyTorch. The ensemble method AdaBoost. The conventional methods are artificial neural network (ANN) support vector machine (SVM), K-nearest neighbors (KNN), decision tree (DT), random forest (RF).

D. Regression Task

As we mentioned in Sec. III, regression is a harder problem, we can see it as a multi-classification with a infinite number of classes. Here, the target is the Generalized Robustness, an entanglement quantifier defined in Eq. (3) and calculated for each sample in our dataset with an ϵ -OEW, and $\epsilon = 10^{-5}$ (cf. Sec. II).

In spite of starting with low-precision target values, and not possessing a huge dataset to fill the infinite classes, autoML still manages to recover a tendency line of the quantifier. The idea here is to use the regression to validate the previous classifiers and estimate the amount of entanglement in the state to some degree. Thus, higher values for the predicted GR can give us confidence about the entanglement of an unknown state.

ML technique	MAE
TPOT	0.0373
AutoKeras	0.0335
Auto-PyTorch	0.0347
ANN	0.0350
SVM	0.0383
KNN	0.0500
DT	0.0649
RF	0.0463

TABLE IV. Different machine learning techniques applied to the dataset and their verified mean absolute error (MAE) on the test set. The autoML techniques are TPOT, AutoKeras, and Auto-PyTorch. The conventional methods are artificial neural network (ANN), support vector machine (SVM), K-nearest neighbors (KNN), decision tree (DT), random forest (RF).

In Tab. IV we have a comparison of different ML techniques for the regression task, with the best model in

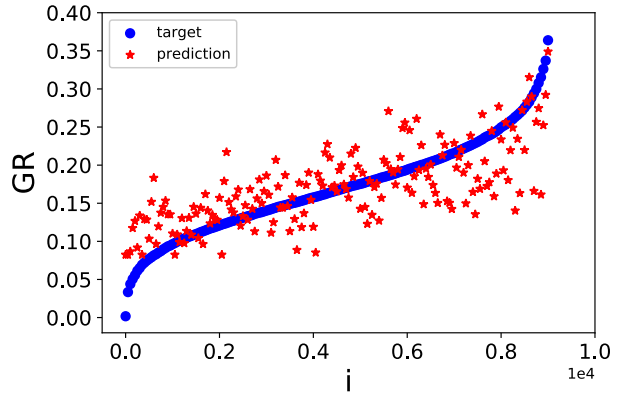


FIG. 4. In blue (circle) the Generalized Robustness (cf. Eq. (3)) and in red (star) the ML prediction considering around 9000 test set points after an autoML model has been trained and deployed with AutoKeras package, with a mean absolute error (MAE) of 0.0335.

boldface. Since Auto-sklearn still very incipient for this task, we chose to remove it from this comparison. The autoML also proved to be efficient in this task, outperforming standard algorithms. To achieve the best performance, AutoKeras had an extra fine-tuning, called *final fit*, which took an extra hour in addition to the 6 hours in our time window. This extra fine-tune was responsible for a reduction of almost 5% in the *Mean Absolute Error* (MAE).

We show the target values (sorted from minimum to maximum) and its corresponding regression using AutoKeras in Fig. 4, with a MAE of $L1 = 0.0335$. For a better plotting experience, we reduced the density of points by a factor of a hundred.

In case we want a model with a more accurate description of the quantifier, one should increase the number of samples in the dataset, so the density of points in each of these infinite classes represents the set accordingly.

Finally, we can establish a threshold in which we can trust the predictions as a function of our achieved MAE. For example, we can define a conservative threshold, $\delta \equiv 3 \times L1 \approx 0.1$, so, when the machine outputs GR greater than δ we say the state is entangled. Note that, for smaller values ($GR < 0.1$), the output is almost an upper-bound, meaning that the true value is smaller than the prediction. On the other hand, for large values ($GR > 0.25$) the predictions establish a lower-bound and the true value is larger than the prediction. For the intermediate region ($0.1 < GR < 0.25$), although we cannot assess upper/lower bounds, it satisfies the criterion to be larger than $\delta = 0.1$, and the state can be said to be entangled.

V. CONCLUSION

In this work, we used Automated Machine Learning (autoML) to successfully classify random quantum states of two qutrits as separable (SEP), PPT entangled state (PPTES), or NPT. We chose a scenario in which we possess enough data to reconstruct ρ via linear system inversion, but no direct measurements of its entanglement. In addition to classification in terms of SEP/PPTES/NPT, we could also estimate the amount of entanglement in the state using autoML for a regression of the Generalized Robustness of Entanglement. In conclusion, if we use both classifiers and the regression, we can decide whether an unknown state is entangled and validate one test using others.

We could successfully apply our framework even in the hardest instance of the problem, when the Peres-Horodecki criterion cannot decide whether a quantum state is separable or entangled with positive partial transposition. With autoML, for the binary (SEP *vs.* PPTES) task, TPOT accurately classified SEP with 74.1% and PPTES with 76.6%, with an overall performance of 75.3%. For the multi-classification (SEP *vs.* PPTES *vs.* NPT), TPOT accurately classified 71.4% of SEP, 62.4% of PPTES and 88.6%, of NPT states, with an overall performance of 73.8%. Finally, we achieved the mean absolute error of 0.0335 for the regression problem with a conservative confidence threshold of $GR_{ML} > 0.1$ for

entanglement assessment and validation of our classifiers.

To achieve models with higher performance in any of the presented tests, one should increase the number of samples. We trained our models with a dataset containing both random and artificial PPTES states (*cf.* Sec II) and we have a strong numerical evidence that artificially created PPTES using the method in Sec. II is a good strategy to overcome the low probability to draw a random PPTES state using the Hilbert-Schmidt measure.

This computational effort can pay off when we can decide the entanglement of a random state efficiently and with high probability. So, a global repository of correctly labeled states could help the community to train better machines and also validate the results, since we would have a larger number of groups working with the same dataset. This could be paramount in real-time applications, like quantum communication protocols.

ACKNOWLEDGMENTS

We acknowledge the financial support by Brazilian agencies CAPES, CNPq, and INCT-IQ (National Institute of Science and Technology for Quantum Information). We also thank SeTIC-UFSC for the computational time in its cluster. AC acknowledges UFAL for a paid license for scientific cooperation at UFRN and the John Templeton Foundation via the Grant Q-CAUSAL No. 61084, the Serrapilheira Institute (Grant No. Serra-1708-15763) and CNPQ (Grant No. 423713/2016 – 7).

-
- [1] P. W. Shor, in *Proceedings 35th annual symposium on foundations of computer science* (Ieee, 1994) pp. 124–134.
 - [2] L. M. Vandersypen, M. Steffen, G. Breyta, C. S. Yannoni, M. H. Sherwood, and I. L. Chuang, *Nature* **414**, 883 (2001).
 - [3] R. Ursin, F. Tiefenbacher, T. Schmitt-Manderbach, H. Weier, T. Scheidl, M. Lindenthal, B. Blauensteiner, T. Jennewein, J. Perdigues, P. Trojek, B. Ömer, M. Fürst, M. Meyenburg, J. Rarity, Z. Sodnik, C. Barbieri, H. Weinfurter, and A. Zeilinger, *Nature Physics* **3**, 481 (2007).
 - [4] A. Vaziri, G. Weihs, and A. Zeilinger, *Physical Review Letters* **89** (2002), 10.1103/physrevlett.89.240401.
 - [5] S. Gröblacher, T. Jennewein, A. Vaziri, G. Weihs, and A. Zeilinger, *New Journal of Physics* **8**, 75 (2006).
 - [6] A. Peres, *Physical Review Letters* **77**, 1413 (1996).
 - [7] M. Horodecki, P. Horodecki, and R. Horodecki, *Physics Letters A* **223**, 1 (1996).
 - [8] M. Horodecki, P. Horodecki, and R. Horodecki, *Physical Review Letters* **80**, 5239 (1998).
 - [9] P. Horodecki, M. Horodecki, and R. Horodecki, *Physical Review Letters* **82**, 1056 (1999).
 - [10] C. H. Bennett, D. P. DiVincenzo, T. Mor, P. W. Shor, J. A. Smolin, and B. M. Terhal, *Physical Review Letters* **82**, 5385 (1999).
 - [11] H.-P. Breuer, *Physical Review Letters* **97** (2006), 10.1103/physrevlett.97.080501.
 - [12] G. Sentís, C. Eltschka, and J. Siewert, *Physical Review A* **94** (2016), 10.1103/physreva.94.020302.
 - [13] P. W. Shor, J. A. Smolin, and A. V. Thapliyal, *Physical Review Letters* **90** (2003), 10.1103/physrevlett.90.107901.
 - [14] L. Gurvits, in *Journal of Computer and System Sciences*, Vol. 69 (2004) pp. 448–484, arXiv:0303055 [quant-ph].
 - [15] L. Gurvits, in *Proceedings of the thirty-fifth annual ACM symposium on Theory of computing* (ACM, 2003) pp. 10–19.
 - [16] R. Horodecki, P. Horodecki, M. Horodecki, and K. Horodecki, *Reviews of modern physics* **81**, 865 (2009).
 - [17] O. Gühne, P. Hyllus, D. Bruß, A. Ekert, M. Lewenstein, C. Macchiavello, and A. Sanpera, *Physical Review A* **66**, 062305 (2002).
 - [18] D. Cavalcanti and M. O. Terra Cunha, *Applied physics letters* **89**, 084102 (2006).
 - [19] T. O. Maciel and R. O. Vianna, *Physical Review A* **80**, 032325 (2009).
 - [20] G. Lima, E. Gómez, A. Vargas, R. Vianna, and C. Saavedra, *Physical Review A* **82**, 012302 (2010).
 - [21] V. Dunjko and H. J. Briegel, *Reports on Progress in Physics* **81**, 074001 (2018).
 - [22] M. Kieferová and N. Wiebe, *Physical Review A* **96** (2017), 10.1103/physreva.96.062327.
 - [23] G. Torlai, G. Mazzola, J. Carrasquilla, M. Troyer,

- R. Melko, and G. Carleo, *Nature Physics* **14**, 447 (2018).
- [24] G. Torlai and R. G. Melko, *Physical Review Letters* **119** (2017), 10.1103/physrevlett.119.030501.
- [25] S. Krastanov and L. Jiang, *Scientific Reports* **7** (2017), 10.1038/s41598-017-11266-1.
- [26] M. August and X. Ni, *Physical Review A* **95** (2017), 10.1103/physreva.95.012335.
- [27] J. Gao, L.-F. Qiao, Z.-Q. Jiao, Y.-C. Ma, C.-Q. Hu, R.-J. Ren, A.-L. Yang, H. Tang, M.-H. Yung, and X.-M. Jin, *Physical Review Letters* **120** (2018), 10.1103/physrevlett.120.240501.
- [28] M. Yang, C. liang Ren, Y. chi Ma, Y. Xiao, X.-J. Ye, L.-L. Song, J.-S. Xu, M.-H. Yung, C.-F. Li, and G.-C. Guo, *Physical Review Letters* **123** (2019), 10.1103/physrevlett.123.190401.
- [29] A. Canabarro, S. Brito, and R. Chaves, *Physical Review Letters* **122** (2019), 10.1103/physrevlett.122.200401.
- [30] A. Canabarro, F. F. Fanchini, A. L. Malvezzi, R. Pereira, and R. Chaves, *Phys. Rev. B* **100**, 045129 (2019).
- [31] I. Goodfellow, Y. Bengio, and A. Courville, *Deep Learning* (MIT Press, 2016) <http://www.deeplearningbook.org>.
- [32] M. Nielsen and I. Chuang, *Quantum Computation and Quantum Information*, 1st ed. (Cambridge University Press, 2000).
- [33] T. Le, W. Fu, and J. Moore, *Bioinformatics* (Oxford, England) (2019).
- [34] M. Feurer, A. Klein, K. Eggenberger, J. Springenberg, M. Blum, and F. Hutter, in *Advances in Neural Information Processing Systems 28*, edited by C. Cortes, N. D. Lawrence, D. D. Lee, M. Sugiyama, and R. Garnett (Curran Associates, Inc., 2015) pp. 2962–2970.
- [35] H. Jin, Q. Song, and X. Hu, in *Proceedings of the 25th ACM SIGKDD International Conference on Knowledge Discovery & Data Mining* (ACM, 2019) pp. 1946–1956.
- [36] H. Mendoza, A. Klein, M. Feurer, J. T. Springenberg, M. Urban, M. Burkart, M. Dippel, M. Lindauer, and F. Hutter, in *AutoML: Methods, Systems, Challenges*, edited by F. Hutter, L. Kotthoff, and J. Vanschoren (Springer, 2018) Chap. 7, pp. 141–156, to appear.
- [37] G. Vidal and R. Tarrach, *Phys. Rev. A* **59**, 141 (1999).
- [38] M. Steiner, *Phys. Rev. A* **67**, 054305 (2003).
- [39] R. J. May, H. R. Maier, and G. C. Dandy, *Neural Networks* **23**, 283 (2010).
- [40] K. Życzkowski, K. A. Penson, I. Nechita, and B. Collins, *Journal of Mathematical Physics* **52**, 062201 (2011).
- [41] K. Życzkowski, P. Horodecki, A. Sanpera, and M. Lewenstein, *Physical Review A* **58**, 883 (1998).
- [42] K. Życzkowski and H.-J. Sommers, *Journal of Physics A: Mathematical and General* **36**, 10115 (2003).
- [43] H.-J. Sommers and K. Życzkowski, *Journal of Physics A: Mathematical and General* **37**, 8457 (2004).
- [44] S. L. Braunstein, *Physics Letters A* **219**, 169 (1996).
- [45] K. Życzkowski and H.-J. Sommers, *Journal of Physics A: Mathematical and General* **34**, 7111 (2001).
- [46] M. Horodecki, P. Horodecki, and R. Horodecki, *Physics Letters A* **283**, 1 (2001).
- [47] F. G. Brandao and R. O. Vianna, *Physical review letters* **93**, 220503 (2004).
- [48] F. G. S. L. Brandão, *Phys. Rev. A* **72**, 022310 (2005).
- [49] A. C. Doherty, P. A. Parrilo, and F. M. Spedalieri, *Phys. Rev. A* **69**, 022308 (2004).
- [50] M. Lewenstein, B. Kraus, P. Horodecki, and J. Cirac, *Physical Review A* **63**, 044304 (2001).
- [51] M. Lewenstein, B. Kraus, J. Cirac, and P. Horodecki, *Physical Review A* **62**, 052310 (2000).
- [52] I. Guyon, L. Sun-Hosoya, M. Boullé, H. J. Escalante, S. Escalera, Z. Liu, D. Jajetic, B. Ray, M. Saeed, M. Sebag, A. Statnikov, W.-W. Tu, and E. Viegas, “Analysis of the automl challenge series 2015–2018,” in *Automated Machine Learning: Methods, Systems, Challenges*, edited by F. Hutter, L. Kotthoff, and J. Vanschoren (Springer International Publishing, Cham, 2019) pp. 177–219.
- [53] P. Mehta, M. Bukov, C.-H. Wang, A. G. Day, C. Richardson, C. K. Fisher, and D. J. Schwab, *Physics Reports* **810**, 1–124 (2019).
- [54] S. Wold, K. Esbensen, and P. Geladi, *Chemometrics and intelligent laboratory systems* **2**, 37 (1987).
- [55] G. A. Seber and C. J. Wild, *New Jersey: John Wiley & Sons* **62**, 63 (2003).
- [56] H. Schütze, C. D. Manning, and P. Raghavan, *Introduction to information retrieval*, Vol. 39 (Cambridge University Press Cambridge, 2008).
- [57] J. Platt, *Sequential Minimal Optimization: A Fast Algorithm for Training Support Vector Machines*, Tech. Rep. MSR-TR-98-14 (1998).
- [58] N. Cristianini, J. Shawe-Taylor, *et al.*, *An introduction to support vector machines and other kernel-based learning methods* (Cambridge university press, 2000).
- [59] J. M. Keller, M. R. Gray, and J. A. Givens, *IEEE transactions on systems, man, and cybernetics*, 580 (1985).
- [60] L. Breiman and J. Friedman, *Classification and regression trees* (1984).
- [61] T. Chen, T. He, M. Benesty, V. Khotilovich, and Y. Tang, *R package version 0.4-2*, 1 (2015).
- [62] K. J. Archer and R. V. Kimes, *Computational Statistics & Data Analysis* **52**, 2249 (2008).
- [63] D. Anderson and G. McNeill, *Kaman Sciences Corporation* **258**, 1 (1992).
- [64] R. Salman and V. Kecman, in *Conference Proceedings - IEEE SOUTHEASTCON* (2012) pp. 1–6.
- [65] R. F. Werner, *Physical Review A* **40**, 4277 (1989).